J. Condensed Matter Nucl. Sci. 38 (2024) 295–306

Research Article

Understanding of MHE Power Generation Patterns by TSC Theory

Akito Takahashi*, Masahiko Hasegawa, Yutaka Mori

MHE Kobe lab Technova Inc., 658–0022 Kobe Japan

Abstract

The main MHE power generation pattern can be explained by the nuclear energy release of 4H/TSC WS fusion events at T-sites of Ni nano-cores. The release occurs when dynamic 4H cluster formations of 4 protons move from O-sites under phonon excitations in GMPW (global mesoscopic potential well) of Ni-nano-islands. This is the major process of power (about 20 W in our runs). In addition, minor excess power (about 4 W) is considered to be continuously released by 4H/TSC WS fusion events at SNHs (sub-nano-holes) on surfaces of Ni-nano-cores. This minor process remains after the H/Ni ratio is saturated. We found a method of MHE power re-activation by the RCV (reaction chamber valve) close-to-open method after H/Ni loading ratio becomes nearer to saturation. When RCV is opened, pulse thermal power generation occurs from 4H/TSC WS fusions at SNHs, which induces H-gas desorption-bursts from T-sites of Ni-nano-cores. This trigger event produces empty T-sites in Ni-nano-cores and slow H-loading to T-sites restarts with relatively large generation of 4H/TSC WS fusion power (10-15 W) for a considerably long time (about one day in our trigger-trial runs). This re-activation/trigger process can be repeated in-situ. We were able to trigger pulse thermal power more than ten times. The prediction by the TSC theory seems to be working very well. Some brief historical aspects of "cold fusion" or MHE research evolution are described in a portion of the Introduction.
 ISSN 2227-3123

Keywords: Metal hydrogen energy, heat pattern, TSC theory, H-loading ratio

1. Introduction

We are convinced by our latest results [1]–[11] that we have now found a very reproducible method of generating high energy density excess thermal power in long lasting reactions, using nano-composite metal meso-catalyst and hydrogen (D or H) gas interaction at elevated temperatures. The original aspect of underlying phenomena was published in our ICCF20 paper [12].

We gave up doing the F-P type electrolysis experiments around 2000, due to the very difficult reproducibility of AHE. We thought that the FPHE (Fleischman-Pons Heat Effect) phenomenon could happen by 4D/TSC formation at arbitrary (by chance) formed surface nano-structure sites (SNH: sub-nano-holes) and/or T-sites in the FCC lattice of Pd (or Ni) metal, [13] conditions which would be difficult create artificially with electrochemical methods. The co-deposition method (P. Boss et al. [17]) surface analysis gave AT (Akito Takahashi) a hint for possible nano-structure

*Corresponding author: E-mail: akito@sutv.zaq.ne.jp

 ISSN 2227-3123

formation. Next, the Arata-Fujita idea [18] of Pd nano-particles in zirconia gave AT a more functional hint to a way to make a working material in a systematic way: the spin technique. We made spin material to do the D-gas-loading experiments with mesoscopic size catalyst powder of Pd- or Ni-core binary nano-composite islands [19]. Pure Pd samples do not have the capability to trap D(or H) particles in lattice sites or surface defects at elevated temperatures (>> 300°C) necessary for an energy source application, therefore we have concentrated on Ni-core/Pd(or Cu)-shell meso-catalyst structures [1]–[16]. According to the 4D(or H)/TSC formation on surface SNHs (or inner sub-periodic potential wells of a global mesoscopic potential well: GMPW) of a nano-island, TS clusters formation are more enhanced the higher the D-loading ratio is in meso-catalyst islands [13], [19]. (We found 3.5 loading at most for PNZ.) We have tried to design PNZ or CNZ type samples of mesoscopic catalysts.

Using our new experimental system (called D-system [9]) of MHE (nano-metal hydrogen energy) reaction, we are able to measure and to evaluate more clearly the anomalous heat effect (AHE) by the elevated temperature interaction of nano-composite metal samples and hydrogen-gas. Two findings of new characteristics of AHE excess power by the MHE reaction are reported [10]. After starting initial heating by W2 (100-160 W) heater, excess thermal power by MHE is steeply generated from around 300°C of CNZ-sample powder in the outer region. Excess power suddenly starts to increase when the H/Ni loading ratio reaches around 1.0. This timing is considered to be the time that H-loading at O-sites of Ni core become full, attaining H/Ni = 1.0 in about 20–60 minutes in our runs (Phase-1 process: Fast H-Loading). After that turning point, relatively high excess power generation continues for about 3 days, until the elapsed time region where H/Ni loading ratio saturates to be far greater than 1.0; H/Ni = 2.2 was the saturated value in some runs. This is the second phase H-loading by T-sites loading in Ni core: (Phase-2 process: Slow H-Loading).

The main MHE power generation pattern can be explained by the nuclear energy release of 4H/TSC WS fusion events at T-sites of Ni nano-cores, by dynamic 4H cluster formation of 4 protons (associating 4 electrons) moved from O-sites under phonon excitations in GMPW (global mesoscopic potential well) of Ni-nano-islands [13], [19]. This is the major process of power (about 20W in our runs). In addition, minor excess power (about 4 W) is considered to be continuously released by 4H/TSC WS fusion events at SNHs (sub-nano-holes) on surfaces of Ni-nano-cores. This minor process remains after the H/Ni ratio is saturated.

We found a method of MHE power re-activation by the RCV (reaction chamber valve) close-to-open method after H/Ni loading ratio becomes nearer to saturation [9], [10]. When RCV is opened, pulse thermal power generation happens by 4H/TSC WS fusions at SNHs, which induces H-gas desorption-bursts from T-sites of Ni-nano-cores. This trigger event produces empty T-sites in Ni-nano-cores and slow H-loading to T-sites restarts with relatively large generation of 4H/TSC WS fusion power (10-15 W) for a considerably long time (about one day in our trigger-trial runs). This re-activation/trigger process can be repeated in-situ. We have successfully triggering it more than ten times.

We have to bear in mind that our latest reports [9], [10] at the JCF-22 Meeting would be shocking to old authorities in CF/LENR studies, which were based on heavy water electrolysis with Pd cathode, and based on ideas of deuteron induced fusion reactions. We were convinced by our characteristics data of a close correlation between excess power evolution and H/Ni loading ratio exceeding 1.0, by the elevated temperature interaction of light hydrogen and mesoscopic nano-metal catalyst. We are also convinced that the results with light hydrogen take place with the same underlying physics mechanism as our former results using deuterium gas and meso-catalyst interaction at room temperature and elevated temperatures [1]–[11]. Both the light hydrogen and deuterium reactions observed appear to match very well with AT's 4H/TSC WS fusion and 4D/TSC fusion theories. The common underlying physics is the condensed cluster fusion (CCF) of hydrogen isotopes in dynamic ordering process of condensed matter (to be mesoscopic catalyst) [7], [13], [16], [20]. So, our results for light hydrogen results are theoretically consistent with the old observations of heavy water/gas and Pd metal interaction. Both results showed energy generation density of more than 1000 times conventional chemical reaction energies, leading us to conclude this is of nuclear origin. We understand we are seeing, at least, one rational solution of the "cold fusion" puzzle. We may hope that other rational solutions may emerge from other efforts. We think we can go ahead to the R&D stage for industrial application to clean portable energy devices of primary nuclear energy source.

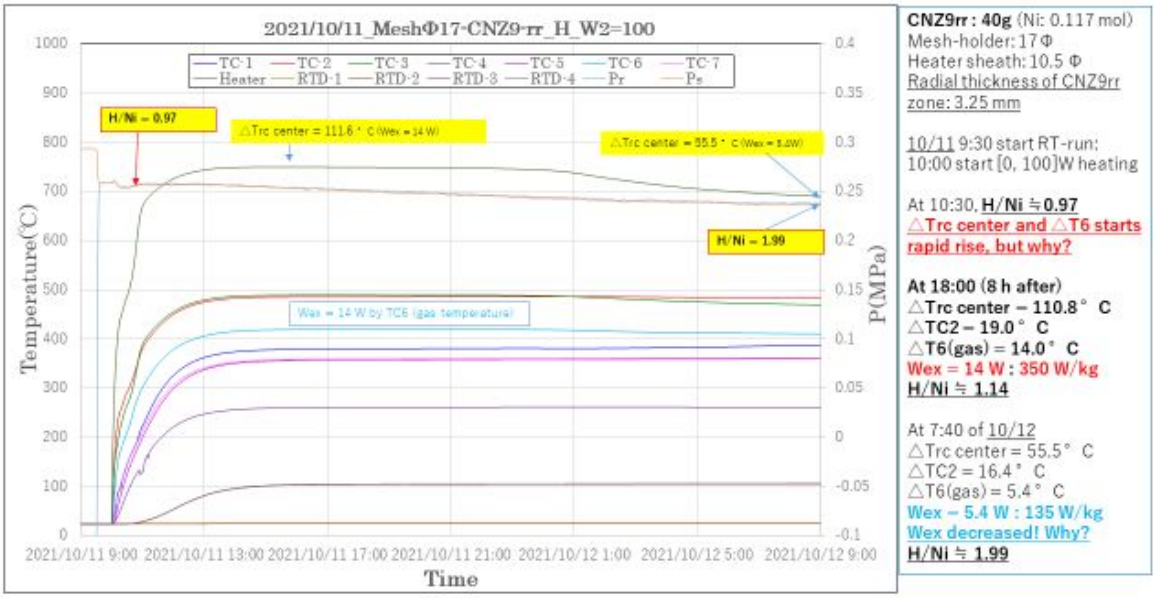

Figure 1. Typical example of raw data from the D-system MHE experiment for re-calcined sample.

2. Correlation between Excess Thermal Power and H/Ni Loading Ratio

A typical example of raw data from the new D-system MHE experiment [9], [10], [21] is shown in Fig. 1. Blank calibration runs were carried out with three dummy samples, namely zirconia beads, zirconia fine powder and a "dead" CNZ7rrr sample. To estimate excess power generation by active sample runs, we found that the blank data of the dead sample is the most accurate for estimating increased temperatures in each point of the D-system. Estimation of excess thermal power by active samples (CNZ9 series and CNZ8 series in this paper) was made by using H2-gas temperature in the reaction chamber (RC) in current data [9], [10].

We have found for every initial ET (elevated temperature) run of CNZ-type samples after re-calcination that excess power rises very steeply when the H-loading ratio (H/Ni) exceeded a value close to 1.0. Relatively high excess power levels (14 W in Fig. 1) plateaued, continuing for many hours (0.5 to 3 days, depending on sample type), and started to decay slowly after saturating H/Ni loading ratios (around 2.0 in real runs). Why did this pattern of excess power evolution occur? We have found also that temperature data at the RC center (Trc-center) was most sensitive to the evolution of excess thermal power generation. However, to estimate excess power, the increment of the H-gas temperature in the RC (ΔT6) from the "dead sample" blank data is appropriate in this study, considering that gas temperature in the RC should reflect the average trend. We have oil mass flow calorimetry data by radiation heat recovery in the D-system. Due to the very slow response of the oil outlet temperature, the present oil mass flow system does not show accurate time evolution data for excess power, but as an estimation of integrated heat over a long run, it is effective.

In Fig. 2, we show a typical example of correlation data between excess thermal power evolution and H/Ni loading ratio evolution. During H/Ni loading, the fast-loading phase reached H/Ni 0.9 in ca. 30 minutes after the W2 heater

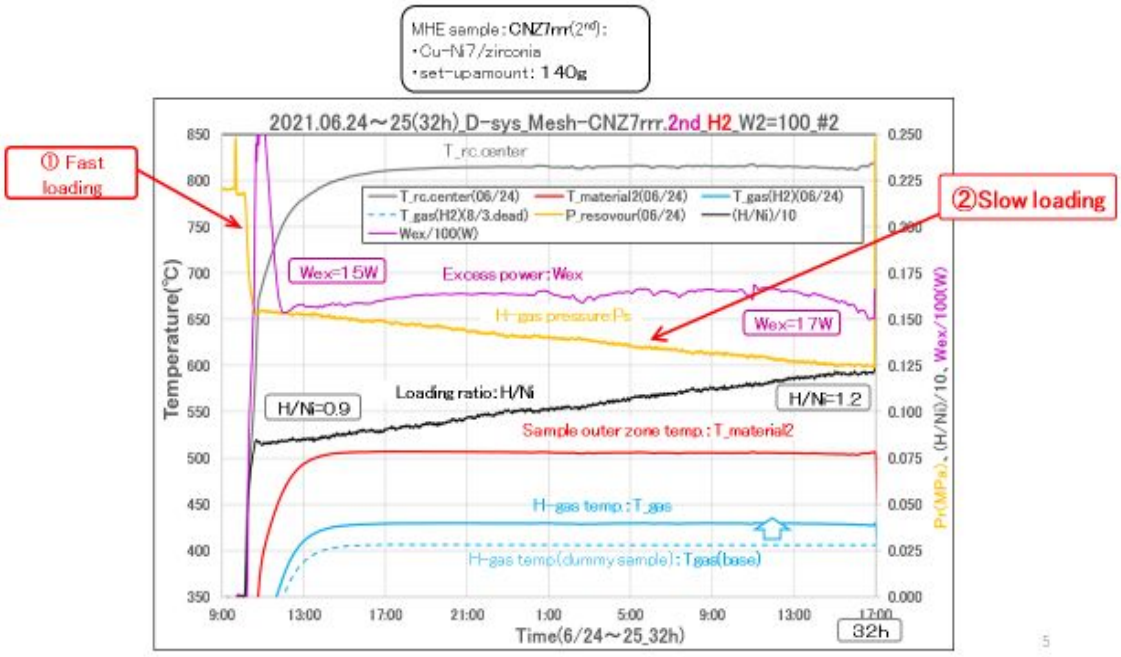

Figure 2. Typical data showing correlation between excess power (W_{ex}) evolution and H/Ni loading ratio evolution, for ET run of CNZ7rrr sample which was still active for the MHE reaction.

was turned on (100 W constant power supply in this case). Following this, the very slow H-loading phase lasting for a few days, reaching the saturated value around 2.0. As for excess thermal power evolution, we see a burst-like peak [3] after the fast H/Ni loading finished and rather plateau-like power level (15-17W) continues with the slow H/Ni loading phase for many hours. Why are such patterns of H/Ni loading and excess power in close correlation?

We have found that H-loading ratio can become very high as 3.5 when we used nano-composite metal particles of Pd and Pd-Ni binary particles in ceramics supporter flakes [19] at room temperature. Here we consider that high H-loading over H/Ni = 1.0 can be formed for Ni-core/Cu-incomplete-shell nano-composite meso-catalyst, especially at elevated temperatures, probably by the endothermic H-absorption process to Ni-core lattice, as shown in the model in Fig. 3. H_2 gas molecules may be trapped first by electron dangling bonds at sub-nano-holes (SNHs) on surface of Ni-core with Cu (defect points), and dissociated to protons to enter into Ni nano-core lattice for occupying octahedral sites (O-sites) of Ni FCC lattice. When all O-sites are occupied by protons, H/Ni loading ratio becomes 1.0. After that fast-loading phase, very slow H-loading to tetrahedral sites (T-sites) of Ni FCC core lattice goes on by excited phonon states of protons at O-sites under elevated temperature condition. As the T-site H-trapping potential is with shallow well on potential hill of FCC structure, efficient excitation of proton oscillator phonon at O-site is needed. The non-linear coupled proton oscillations to produce high phonon states can be expected in the global mesoscopic potential well (GMPW) with inner fine FCC Bloch potentials of O-sites, under elevated temperatures [19]. Maximum partial loading ratio to T-sites is 2.0. Total loading to be saturated is therefore 3.0 as sum of O-sites and T-sites H-occupations, theoretically. The experimentally observed value 0.9 in Fig. 2 can be regarded as 1.0 nominal value,

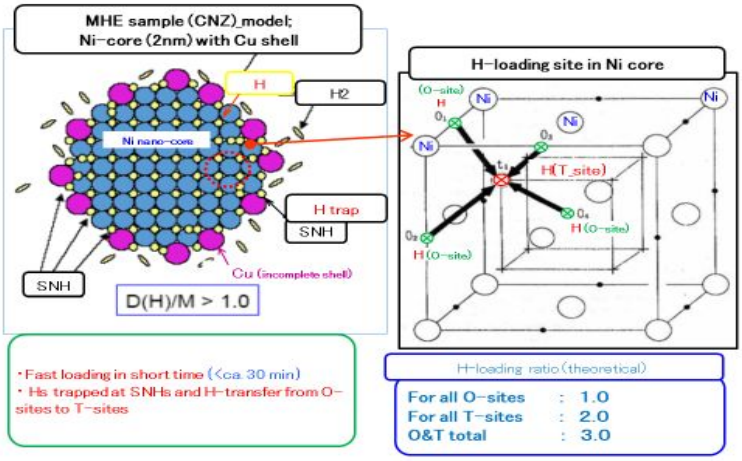

Figure 3. Model of hydrogen loading to a Ni-core/Cu-incomplete-shell nano-composite meso-catalyst particle [13], [19].

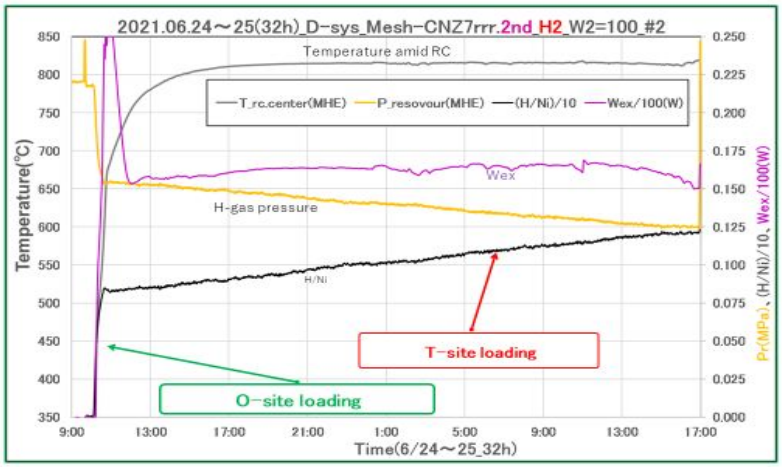

Figure 4. Explanation of two (fast and slow) phase H-loadings to Cu_1Ni_7/zirconia nano-composite sample powders, in close correlation with Wex (excess thermal power).

namely we conceive 90% meso-catalyst state of CNZ7rrr sample, and we know that bulk Ni metal sample cannot absorb Hs over 1.0.

As shown in Fig. 4, the observed H-loading patterns with excess thermal power correlation can be explained as the O-site H-loading for the fast-loading phase and the T-site H-loading for the slow loading phase. The next question is why the excess power pattern correlates closely to the evolution of H/Ni loading ratio.

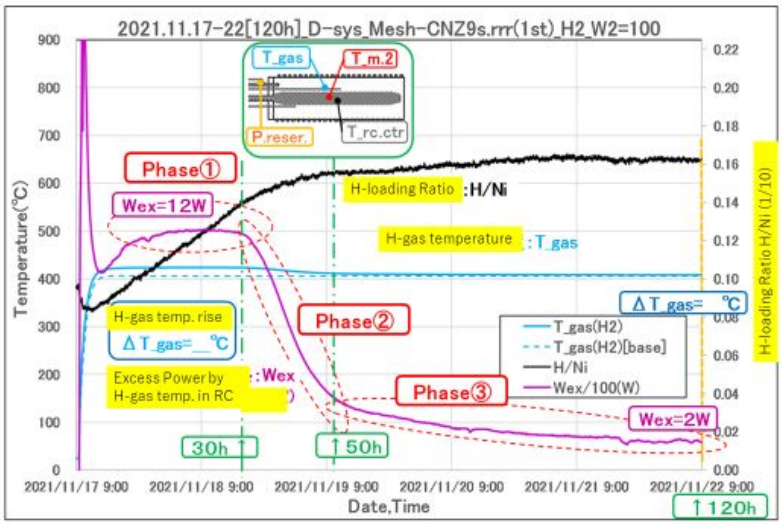

Figure 5. Evolutional correlation of H/Ni loading ratio and excess thermal power, with a typical example of a CNZ9srrr sample (140 g) after the third re-calcination (rrr).

In Fig. 5 a typical three phase pattern of excess power generation is shown in correlation with H/Ni loading ratio evolution. Explanation by the 4H/TSC WS fusion theory (7, 13, 16) is shown in the flow chart in Fig. 6. The many hours lasting plateau of relatively high power level in Phase-1 is conceived to be produced by the 4H/TSC WS fusion reactions at T-sites. Under full O-sites occupation with protons, 4H-cluster formation probability is enhanced by high order proton-oscillation phonon in GMPW of Ni-nano-core. If the end-state oscillation of 4H/TSC condensation collapse continues more than 1.0 fs, about 3% of 4H/TSC will produce the nuclear energy of WS fusion, as shown in a simple simulation scheme (Fig. 7) [16]. Detailed data of a simulation of 4H/TSC end-state oscillation is shown in [7].

When the density of remaining empty T-sites rapidly decreases as the H/Ni loading approaches saturation. 4H/TSC WS fusion rates also decrease accordingly. This is Phase-2 of Fig. 5. After the saturated occupation of T-sites, smaller level of 4H/TSC WS fusion rates may continue at SNHs of Ni-nano-cores. This is Phase-3 of Fig. 5.

In Fig. 8, we show that heat vs. H/Ni correlation patterns are reproducible for changing samples and heating conditions. Total heat energy by excess thermal power plateau by this 160 W run is 12.6 MJ/mol-H, which is equivalent to the specific reaction energy of 131 eV/H-atom-absorbed, for 70 h duration. We know that H-absorption to CNZ sample at elevated temperature is endothermic. However, even if we assume that H-absorption is an exothermic reaction, 131 eV/H-atom-absorbed is too large in 2–3 orders of magnitude to be a chemical reaction, and we must conclude it has a nuclear origin. A very important physics issue is that light hydrogen can generate fusion-like nuclear energy in a laboratory experimental system. By assuming 4H/TSC WS fusion, 68 ppm H atoms would be consumed by the nuclear reaction to produce MHE excess heat in this case.

However, why have we observed larger and longer “high-power plateau” with higher H/Ni saturated value with the 160 W heating case than the 100 W case?

For the H/Ni>1.0 condition, phonon-excited movement of protons (Hs) from 4 O-sites to a T-site has the highest probability for one H, and lower probabilities for 2H, 3H and 4H, in relative order, when the Ni-core temperature is lower. T-site occupation of Hs is most enhanced in the lower temperature condition. Fig. 9 shows the enhancement of

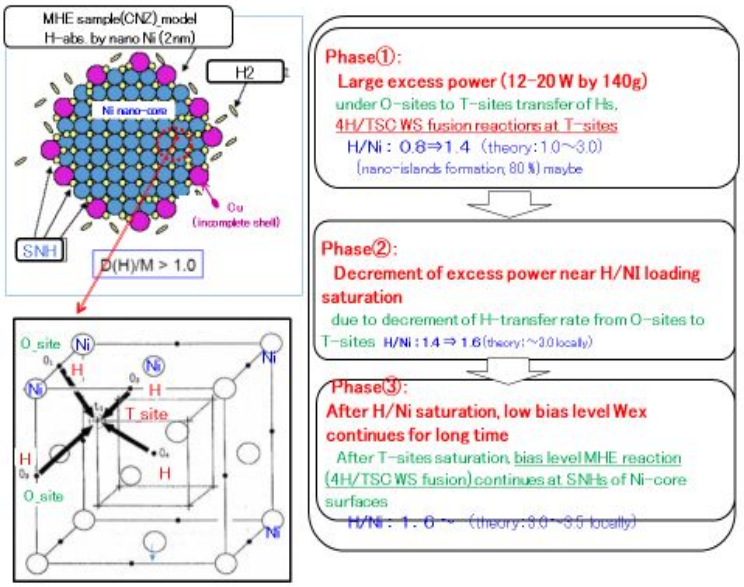

Figure 6. Explanation schematic of MHE power generation patterns with evolution of H/Ni loading ratio.

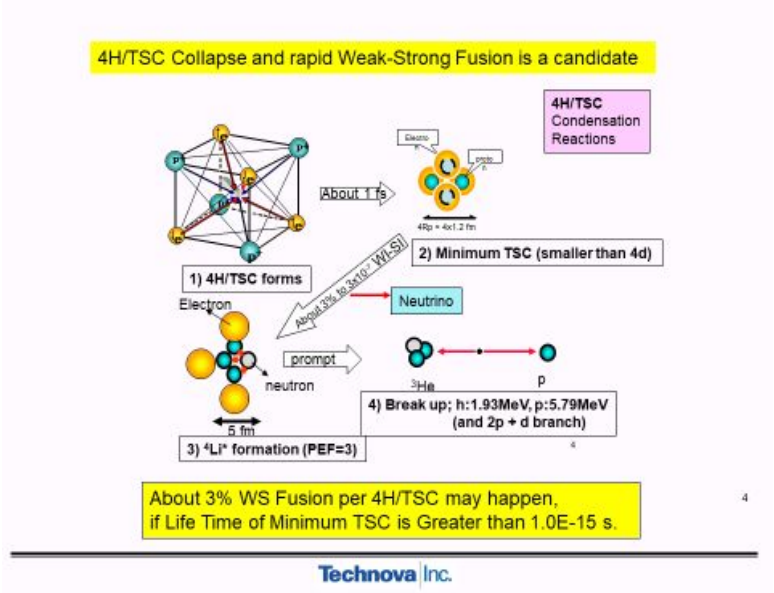

Figure 7. Simplified scheme of 4H/TSC WS fusion model [7], [16].

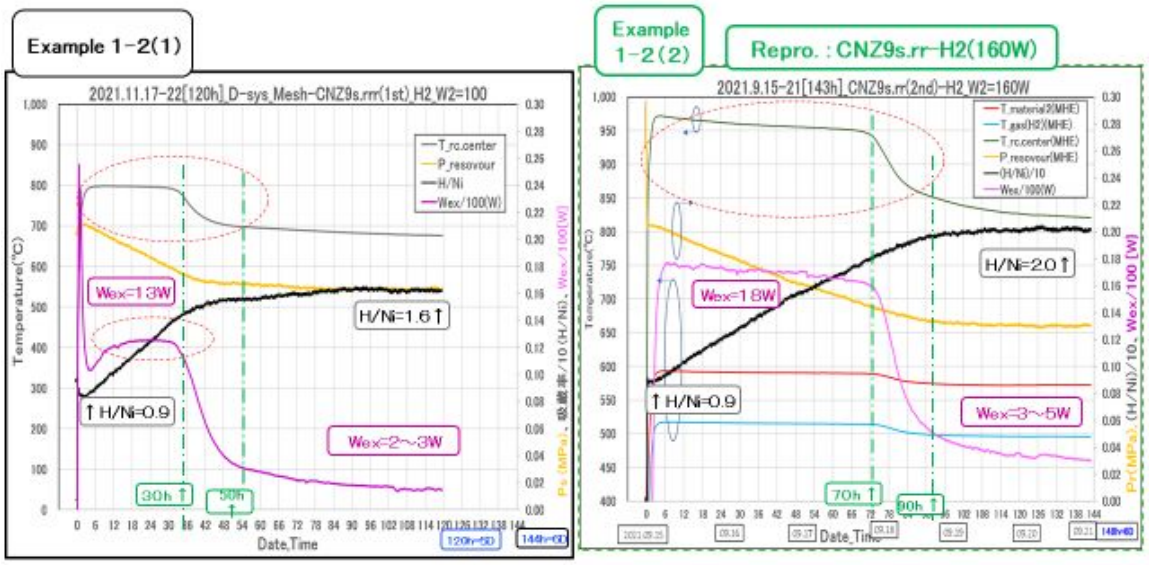

Figure 8. Comparison of power generation patterns for the lower (100 W) heating and the higher (160 W) conditions, with H/Ni loading patterns.

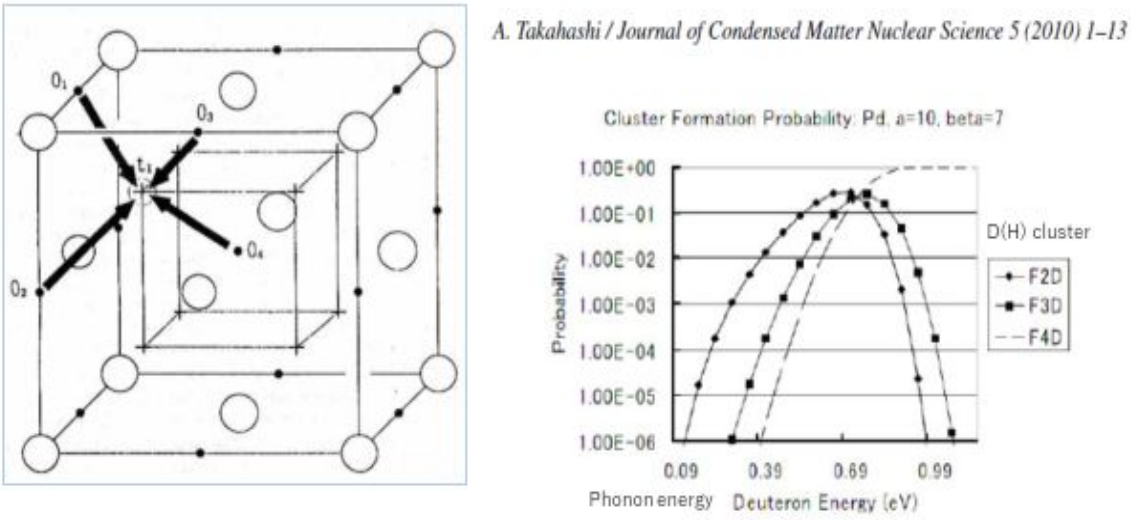

Figure 9. Competition of H-cluster formation probabilities under the FCC lattice proton phonon excitation energy [22].

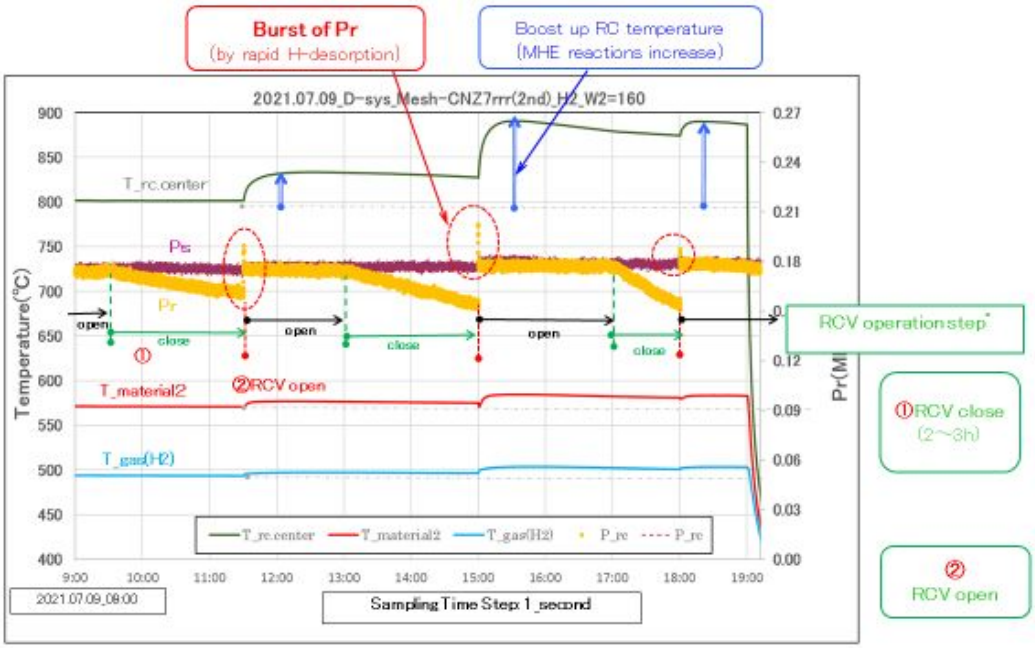

Figure 10. Re-activation data of MHE power by the RCV-close-to-open method [9], [10], [21].

the H-cluster formation probability by the phonon excitation level. Namely, 4H/TSC WS fusion rate at T-sites becomes more enhanced at higher temperatures for O-site phonon excitation, for the H/Ni > 1.0 condition. T-sites will remain empty after 4H/TSC WS fusion events. Therefore, it takes the condition that the more time for full T-site occupation with Hs needs when the 4H/TSC WS fusion rate is higher. As a consequence, integrated excess heat by MHE reactions can be enhanced by higher W2 heater condition. However, how large W2 watts can be supplied is the actual problem. However, we observed that duration of "high Wex plateau" changed by changing samples (by changing Cu/Ni atomic ratio and frequency of re-calcination) [21].

3. Triggering Mechanism of MHE Power Re-Activation

We have found the MHE re-activation method by the RCV-close-to-open method [9], [10]. Before reaching the saturation of H/Ni value (close to 2.0 in real runs), we may close the RC gas valve and wait for several hours.

We observe an H-gas pressure decrease (brown-color data in Fig. 10) during the closure of RCV (reaction chamber valve), showing slow H-absorption by CNZ sample. When we opened the RCV, a burst of Pr (H-pressure of RC) and boost-up of RC temperatures were recorded, which showed an increase of MHE power, which is to say re-activation. After the triggering by RCV-opening, the boosted-up excess power (15-10 watts in the run) continued for many hours. By repeating the RCV-close-to-open treatments, we observed a boost-up of excess power level repeatedly. What is the mechanism of this triggering/activation phenomenon?

When RCV is closed, H_2 accumulated on SNHs, moving from Ni-core inside. When RCV is opened, incoming H_2 meets accumulated H_2 to generate 4H/TSC to WS fusion, which generates a heat burst, and an H-desorption burst

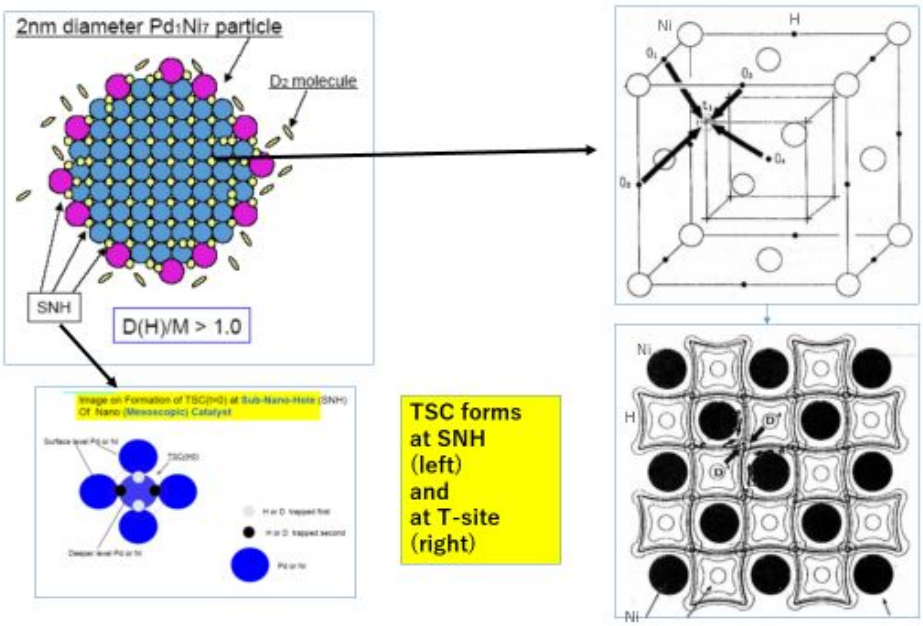

Figure 11. 4H/TSC WS fusion events can take place at surface SNHs (lower left figure) and also at T-sites of Ni-nano-core FCC lattice sites (right figure).

is induced. (See the left side of Fig. 11.) After H/Ni exceeds 1.0, absorbed Hs slowly fill T-sites by H-moving from surrounding 4 O-sites under phonon excitation (Fig. 11, right lower). The 4H/TSC WS fusion rate will be enhanced at T-sites under this process. When all T-sites will be filled with Hs, 4H/TSC formation rates will drop. By RCV-close-open triggering with H-desorption burst, empty T-sites will be generated, and the process of the slow phase H-loading at T-sites restarts, generating 4H/TSC WS fusion events.

4. Concluding Remarks

1) After starting initial heating by W2 (100 – 160 W) heater, excess thermal power by MHE is steeply generated from around 300°C outer region temperature of CNZ-sample powder.
2) Excess power suddenly starts to increase when the H/Ni loading ratio reaches around 1.0. This timing is considered to be the time that H-loading at O-sites of Ni core becomes full, attaining H/Ni =1.0 in about 20–60 minutes in our runs (Fast Loading process).
3) After that turning point, relatively high excess power generation continues for 1- 4 days, until the elapsed time region where H/Ni loading ratio saturates to be far greater than 1.0; H/Ni = 2.2 was the saturated value in some runs. This is the second phase H-loading by T-sites loading in Ni core: (Slow Loading process).
4) MHE power generation can be explained by the nuclear energy release of 4H/TSC WS fusion events at T-sites by dynamic 4H cluster formation of 4 protons moved from O-sites under phonon excitations in GMPW (global mesoscopic potential well) of Ni-nano-islands. This is the major process of power (about 20W in our experimental runs). In addition, minor excess power (about 4 W or less) is considered to be continuously

released by 4H/TSC WS fusion events at SNHs (sub-nano-holes) on surface of Ni-cores. This minor process remains after H/Ni ratio is saturated.

5) We found a method of MHE power re-activation by the RCV (reaction chamber valve) close-to-open method after H/Ni loading ratio becomes nearer to saturation. When RCV is opened, pulse thermal power generation occurs by 4H/TSC WS fusion at SNHs, which induces H-gas desorption-bursts from T-sites of Ni-cores. This trigger event produces empty T-sites in Ni-cores and the slow H-loading to T-sites restarts with relatively large generation of 4H/TSC WS fusion power (10-15 W) for a considerably long time (about one day in present trigger-trial runs). This re-activation/trigger process can be repeated.
6) Predictions by the TSC theory seem to be working very well.

References

[1] Akira Kitamura, Akito Takahashi, Koh Takahashi, Reiko Seto, Takeshi Hatano,Yasuhiro Iwamura, Takehiko Itoh, Jirohta Kasagi, Masanori Nakamura, Masanobu Uchimura, Hidekazu Takahashi, Shunsuke Sumitomo, Tatsumi Hioki, Tomoyoshi Motohiro, Yuichi Furuyama, Masahiro Kishida, Hideki Matsune; "Excess heat evolution from nanocomposite samples under exposure to hydrogen isotope gases", *Int. J. Hydrogen Energy*, **43** (2018) 16187–16200

[2] Yasuhiro Iwamura, Takehiko Itoh, Jirohta Kasagi, Akira Kitamura, Akito Takahashi, Koh Takahashi, Reiko Seto, Masanobu Uchimura, Hidekazu Takahashi,Tatsumi Hioki, Tomoyoshi Motohiro, Yuichi Furuyama, Masahiro Kishida, Hideki Matsune, "Anomalous Heat Effects Induced by Metal Nano-composites and Hydrogen Gas", *J. Condensed Matter Nucl. Sci.*, 29, 119–128 (2019)

[3] Toyoshi Yokose, Akito Takahashi, Koh Takahashi, Yuichi Furuyama, "Anomalous Heat Burst by CNZ7 Sample and H-Gas", Proceedings of JCF19, pp. 18–35, 2019

[4] Akito Takahashi, Toyoshi Yokose, Yutaka Mori, Akira Taniike, Yuichi Furuyama, Hiroyuki Ido, Atsushi Hattori, Reiko Seto, Atsushi Kamei, Joji Hachisuka, "Latest Progress in Research on AHE and Circumstantial Nuclear Evidence by Interaction of Nano-Metal and H(D)-Gas", *J. Condensed Matter Nucl. Sci.*, 33, 14–32, 2020

[5] Akito Takahashi, Toyoshi Yokose, Yutaka Mori, Akira Taniike, Yuichi Furuyama, Hiroyuki Ido, Atsushi Hattori, Reiko Seto, Atsushi Kamei, Joji Hachisuka, "Enhancement of excess thermal power in interaction of nano-metal and H(D) gas", Proc. JCF20, pp. 9–27, 2020

[6] Masahiko Hasegawa, Yutaka Mori, Akito Takahashi, Joji Hachisuka, Hiroyuki Ido, Reiko Seto, Akira Taniike, Yuichi Furuyama, "Comparison of AHE data between H2 and He runs for CNZ7rrr Sample", Presentation at JCF21 Meeting, December 2020, web conference of JCFRS: (PDF) Comparison of AHE data between H2 and He runs for CNZ7rrr sample - English version (researchgate.net)

[7] Akito Takahashi, "4H/TSC Effective Life Simulation rev2"; see (PDF) 4H TSC End State Effective Life Simulation 2rev (researchgate.net)

[8] Akito Takahashi, Fundamental of Rate Theory for CMNS, J. Condensed Mat. Nucl. Sci., 1–18, 19 (2016) (PDF) Fundamental of Rate Theory for CMNS (researchgate.net)

[9] Yutaka Mori, Akito Takahashi, Masahiko Hasegawa, Joji Hachisuka, Yuichi Furuyama; New MHE Experiments by D-System, JCF-22 Meeting, March 2022, see also: (PDF) New MHE Experiments by D-System (researchgate.net)

[10] Masahiko Hasegawa, Akito Takahashi, Yutaka Mori, Joji Hachisuka, Yuichi Furuyama, Characteristics of Excess Power Generation in MHE Experiments by D-System, JCF-22 Meeting, March 2022, see also: (PDF) Characteristics of Excess Power Generation in MHE Experiments by D-System (researchgate.net)

[11] (PDF) MHE nuclear-like thermal power generation and guiding TSC theory (researchgate.net)

[12] (2) (PDF) Anomalous Heat Effects by Interaction of Nano-Metals and H(D)-Gas (researchgate.net)

[13] Akito Takahashi, Physics of Cold Fusion by TSC Theory, J. Condensed Mat. Nucl. Science, 13, 565–579, (2013) (PDF) Physics of Cold Fusion by TSC Theory full paper (researchgate.net)

[14] Akito Takahashi, Nuclear Products of Cold fusion by TSC Theory, J. Condensed Mat. Nucl. Science, 15, 11–22, (2014) (1) (PDF) Nuclear Products of Cold Fusion by TSC Theory (researchgate.net)

[15] Akito Takahashi, The Basics of Deuteron-Cluster Dynamics as Shown by a Langevin Equation, J. Marwan and S. Krivit Ed., Low-Energy Nuclear Reactions and New Energy Technologies Sourcebook Volume 2, Chapter 11 (pp.193-217), ACS Symposium Series 1029, 2009 (1) (PDF) Basics of Deuteron-Cluster Dynamics by Langevin Equation (researchgate.net)
[16] Akito Takahashi, Chaotic End-State Oscillation of 4H/TSC and WS Fusion, Proc. JCF-16, 41–65 (2016) (1) (PDF) Chaotic End-State Oscillation of 4H/TSC and WS Fusion (researchgate.net)
[17] Pamela A. Mosier-Boss, Frank E. Gordon and Lawrence P.G. Forsley, Characterization of Neutrons Emitted during Pd/D Co-deposition, JCNMS, Vol.6 (2012)13
[18] Y. Arata and Y. Zhang, J. High Temp. Soc., Special Issue, Vol1, 2008
[19] A. Takahashi et al., Mesoscopic catalyst and D-cluster fusion, Proc. JCF11, pp. 47–52, JCFRS web-site, (2011)
[20] Akito Takahashi, Background of Condensed Cluster Fusion, Proc. JCF-15, 63–90 (2015) (PDF) Background for Condensed Cluster Fusion (researchgate.net)
[21] Masahiko Hasegawa, Akito Takahashi, Yutaka Mori, Yuichi Furuyama, MHE Reactions in New Experiments by D-System, paper to ICCF24, July 25–28, 2022, USA
[22] Akito Takahashi, Progress in Condensed Cluster Fusion Theory, JCNMS, 5, 1–13 (2010)

This paper is for Proceeding of ICCF24, July 25-28, 2022, USA, to be submitted to J. Condensed Matter Nuclear Science